THE GEOLOGICAL SOCIETY OF AMERICA®

Stick-split mechanism for anthropogenic fluid-induced tensile rock failure

Mirko van der Baan[1]*, David W. Eaton[2], and Giona Preisig[3]
[1]Department of Physics, University of Alberta, Edmonton, Alberta T6G 2G7, Canada
[2]Department of Geoscience, University of Calgary, Calgary, Alberta T2N 1N4, Canada
[3]Geological Engineering, Department of Earth, Ocean and Atmospheric Sciences, The University of British Columbia, Vancouver, British Columbia V6T 1Z4, Canada

ABSTRACT

Fluids play a critical role in natural and human-induced rock failure. It is unclear, however, if propagation of a tensile fracture is inherently an episodic or continuous process. For example, typical average propagation speeds of hydraulic fracture tips on the order of 1–10 m/min suggest continuous crack growth, possibly at subcritical stress intensities. In contrast, using field observations and numerical and mathematical analyses, we show that fracture growth due to anthropogenic hydraulic fracturing is most likely to occur in an episodic fashion, characterized by stick-split behavior that is analogous to stick-slip motion of earthquakes. The stick-split mechanism is regulated by cyclic variations in fluid pressure near the crack tip, in which each successive failure produces a local pressure drop that temporarily halts or slows fracture propagation. A pressure drop results in partial fracture closure, producing noncontinuous fracture propagation through a process that is reminiscent of hand clapping. Rupture speeds for individual failure events are on the order of the shear-wave velocity of the medium; thus, continuous crack growth is not a likely mechanism for anthropogenic hydraulic fracturing treatments despite slow average tip propagation speeds.

INTRODUCTION

Current mathematical models for propagation of anthropogenic hydraulic fractures (Adachi et al., 2007) generally assume continuous fracture growth. Such models may not accurately reflect the fine details of fracture propagation that occur in nature. In particular, it is commonly assumed that the fluid flow speed at the crack tip matches the fracture propagation velocity, a necessary condition to achieve continuous fracture growth.

A cursory look at two different field observations, namely injection pressure during anthropogenic hydraulic fracturing treatments and growth rate of the resulting microseismic clouds, seemingly supports this view. In a typical treatment stage, fluid pressure generally builds up quasi-linearly with time until the breakdown pressure is reached, after which pressure drops to a roughly constant level called the fracture-propagation pressure (Zoback, 2007). The typical absence of conspicuous cyclical pressure fluctuations during propagation could be interpreted as indicative of continuous fracture growth.

Hydraulic fracturing treatments lead to repeated brittle failure, yielding microseismic events (Cipolla et al., 2011; van der Baan et al., 2013). The microseismic cloud is generally thought to encapsulate the hydraulic fracture (zone). Its growth thus provides an upper bound for the average tip propagation velocity. Commonly, the maximum cloud size increases with the square root of time (Shapiro et al., 1997), again suggesting continuous growth.

The temporal evolution of the microseismic cloud indicates typical fracture growth rates on the order of 1–10 m/min (0.02–0.2 m/s). These are orders of magnitude below the shear-wave velocity. Such rupture velocities are more commonly associated with subcritical crack growth, e.g., due to stress corrosion, generally thought to occur continuously (Anderson and Grew, 1977; Atkinson and Meredith, 1987).

Conversely, there is abundant geologic evidence from outcrops that joints due to natural hydraulic fracturing can be created in both continuous and episodic fashions (Bahat and Engelder, 1984; Lacazette and Engelder, 1992; Davis et al., 2011). In joints, episodic growth is inferred from the existence of ribs and rhythmic plume patterns, implying that the failure front significantly slowed down or temporarily halted (Fig. 1).

Here, we postulate that growth of anthropogenic, fluid-induced tensile cracks generally occurs in an episodic fashion, exhibiting a similar behavior to that of some natural joints in rocks. We refer to this phenomenon as stick-split growth, analogous to stick-slip faulting in earthquakes (Brace and Byerlee, 1966), in that the rupture front temporarily sticks to a specific spot before the surrounding intact rock is once again split by the propagating fracture. We provide seismological evidence to support this as well as additional confirmation by geomechanical modeling and mathematical analysis.

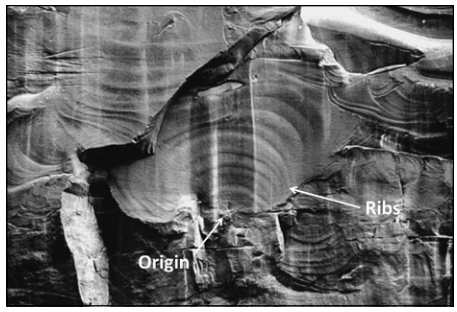

Figure 1. Elliptical joint surface exposed in wall of Navajo Sandstone (Jurassic; southwest United States). Height of cliff face is 8 m. Nested curved lines are ribs. Ribs record position of front of propagating joint at different points in time. Initial rupture point is situated at bottom as ribs are concentrically spreading out from this point. Ribs imply that joint was not created in single failure but that rupture front repeatedly halted or slowed down. Photograph by G.H. Davis. Adapted from Davis et al. (2011), and reproduced with permission.

STICK-SPLIT MODEL

Our proposed model for anthropogenic hydraulic fractures is based on Secor's (1969) model for natural hydraulic fractures. Given the large fluid injection pressures, we assume that fracture propagation is driven by tensile failure at the tip, in response to a fluid pressure that exceeds the tensile rock strength plus the minimum lithostatic stress, i.e., Griffith's criterion (Zoback, 2007; Davis et al., 2011). The fluid pressure at the fracture tip is determined by the injection pressure and the total fracture volume. When local failure occurs, the system volume abruptly increases due to fracture extension, allowing fluid flow toward the new tip location. This is accompanied by a temporary local drop in fluid pressure, most prominently near the fracture tip (Fig. 2). The fracture then partially closes near its tip, until fluid pressure builds up again due to continued fluid injection, repeating

*E-mail: Mirko.vanderBaan@ualberta.ca

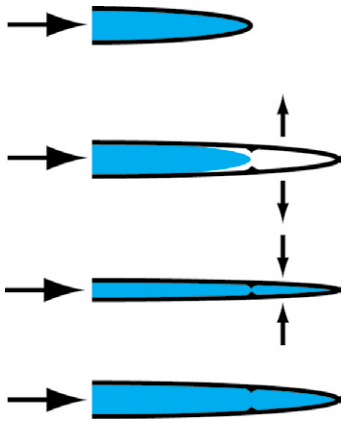

Figure 2. Schematic representation of episodic fracture growth. From top to bottom: (1) Fluid pressure builds up, increasing aperture (stick). (2) Effective pressure exceeds tensile rock strength, causing tensile failure (split), fracture extension, and volume increase. (3) Volume increase causes drop in fluid pressure, partially closing fracture again a split second later. Visual opening-closing movement of fracture walls resembles clapping of hands. (4) Fluid pressure builds up again and process repeats but not necessarily at regular intervals due to variations in local tensile strength and rupture lengths. Ribs are created each time rupture front temporarily halts, possibly due to precipitation of minerals but more likely as remnants of fracture tips.

the cycle of episodic stick-split failure (Secor, 1969; Lacazette and Engelder, 1992). Repeated episodes of abrupt opening of the hydraulic fracture walls, followed by partial closing, is reminiscent of hand clapping (Fig. 2).

Appendix DR1 in the GSA Data Repository[1] provides a mathematical analysis of Secor's (1969) model and of an alternative model that invokes a fluid-free zone near the crack tip (Aki et al., 1977). Both models imply episodic (jerky) growth for anthropogenic hydraulic fracture treatments. Appendix DR1 also details necessary conditions for continuous growth at critical stress intensities.

[1]GSA Data Repository item 2016167, Table DR1 and Appendices DR1 and DR2, is available online at www.geosociety.org/pubs/ft2016.htm, or on request from editing@geosociety.org or Documents Secretary, GSA, P.O. Box 9140, Boulder, CO 80301, USA.

SEISMOLOGICAL EVIDENCE

Seismic field observations provide supporting evidence for the proposed stick-split mechanism. In contrast to shear events, initial opening of a tensile crack is expected to produce a non-double-couple focal mechanism with predominantly positive compressional first motions (Vavryčuk, 2011). Furthermore, tensile events are relatively depleted in S-wave emissions (Foulger and Long, 1984; Eaton et al., 2014c); for a binary system (i.e., tensile or shear), S-wave/P-wave amplitude ratios <5 are indicative of tensile rupture at a 90% level of confidence (Eaton et al., 2014c).

The pressure drop following tensile opening may cause a second seismic event with opposite first-arrival polarity (Foulger and Long, 1984), representing the second part of the hydraulic hand-clapping mechanism. The relatively short time interval between opening and closing (a few milliseconds) generally precludes direct observation of distinct waveform arrivals, but results in a distinctive modulation in the source spectrum (Walter and Brune, 1993; Eaton et al., 2014c). The frequency spectrum for tensile failure is similar to that of a shear-failure event and can be described by a variant of Brune's source model (Walter and Brune, 1993). The spectrum from two co-located events of opposite polarity but separated by some time interval results in a series of periodic notches in the frequency spectrum, with a periodicity that is inversely proportional to separation time.

A microseismic field experiment in British Columbia, Canada (Eaton et al., 2013), conducted during a hydraulic fracturing treatment, included a set of events that are characterized by tensile failure and hydraulic clapping (Eaton et al., 2014c). Of 17 events with S/P amplitude ratio <5, considered indicative of tensile failure, four also display quasi-periodic notches in their spectra. Another hydraulic fracturing treatment in central Alberta, Canada (Eaton et al., 2014a), furnishes further examples of microseismic events that are characterized by both a significant component of tensile failure and source complexity, consistent with a hydraulic clapping mechanism. Appendix DR2 provides details on the processing strategy for both data sets.

Figure 3 shows an inferred tensile event with an S/P amplitude ratio of <2. Both its P- and S_{fast}-wave source spectra display quasi-periodic notches. The spectra are computed by separating the recorded wavefield into constituent wave types (P, S_{fast}, and S_{slow}), beam-forming to enhance the signal-to-noise ratio, and application of a 200 ms Hanning window centered on the wave arrival. As illustrated by the dashed curve for the best-fit model, the spectral notches can be explained by two events with opposite polarity, a composite magnitude of –0.89, a temporal separation τ of 14.5 ms, and fracture radius of 1.1 m and aperture of 1.1 mm. The composite magnitude and temporal separation τ are estimated using the methodology of Eaton et al. (2014c). Estimates for the fracture radius and aperture are obtained using a net pressure of 10 MPa, a shear modulus of 9.7 GPa, and Equations DR2-1 and DR2-2 in Appendix DR2.

We thus interpret this event as opening and subsequent closing of a tensile fracture, where quasi-periodic notches in both the P- and S_{fast}-wave spectra are explained by the hand-clapping mechanism. Both the tensile opening and closing, and any additional shearing, are likely to enhance the extent of the process zone (Rubin, 1993; Davis et al., 2011) in front of the fracture, facilitating subsequent failure. An alternative interpretation for the existence of spectral

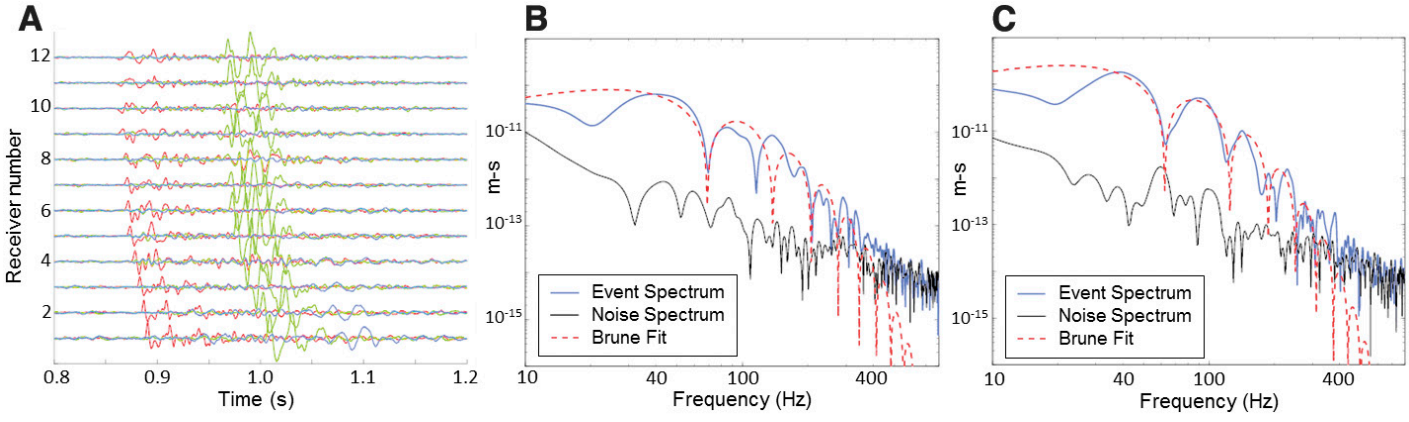

Figure 3. Source spectra of tensile microseismic event, characterized by complex spectral shape with amplitude modulation. A: Recorded waveforms of P- (red), S_{fast}- (green), and S_{slow}-waves (blue). B,C: Displacement (blue) and noise (black) spectra for respectively P-wave (B) and S_{fast}-wave (C) source spectra. Dashed red curves show best-fitting tensile opening-closing model. Black curve shows background noise based on a pre-event noise window. Signal amplitude is above noise level from 10 to 400 Hz.

notches in the S_{fast}-wave spectrum due to successive shear-slip events of opposite polarity is unphysical, as it would require one event to slip in direct opposition to the in situ stress field. Likewise, the possibility that the spectral notches are caused by path effects or receiver-side heterogeneities is unlikely, as spectral notches would then be expected for most recorded events.

MODELING SUPPORT

We use a two-dimensional discrete-element method (Cundall, 1988) to confirm the existence of the stick-split and clapping mechanisms. A rock mass 200 m wide by 170 m high is considered at a depth of 1330 m, with a network of non-persistent natural fractures interconnected with intact rock bridges (incipient fractures). The stress field is characterized by a thrust-faulting regime, with vertical and horizontal principal stresses of, respectively, 42 MPa and 73 MPa. A vertical injection well in the center injects fluids over a 2 m open interval with a three-dimensional–equivalent flow rate of 400 L/min into an initially dry rock (model 1 of Preisig et al., 2015). Figures 4A and 4B show the model layout and setup. Preisig et al. (2015) provide full details on the modeling strategy. Table DR1 in the Data Repository contains the mechanical and hydraulic parameters. Chosen parameters reflect in situ conditions in an underground mine in New South Wales, Australia.

The rock mass is discretized such that intact blocks are bounded by a pre-defined fracture network composed of (1) preexisting natural discontinuities and (2) incipient discontinuities having intact rock properties until rupture. Fluid flow within the propagating fracture significantly exceeds flow into the rock matrix such that poroelastic effects within intact rock can be neglected. This assumption is reasonable for the low-permeability and low-porosity rocks commonly encountered in anthropogenic hydraulic fracturing treatments (Zoback, 2007; Cipolla et al., 2011; van der Baan et al., 2013). The rock matrix is thus considered impermeable in the coupled hydromechanical model; fluids can only flow within the fractures once opened by failure of the pre-defined network of discontinuities.

Figures 4A and 4B show two snapshots of fluid pressure, immediately before and after a failure event. At the fracture tip, fluid pressures are significantly higher before tensile failure than following the expansion, thereby supporting the stick-split model (Fig. 2). The failure event leads to a pressure drop of 8 MPa, a dislocation of 3 m (source radius of 1.5 m), and an aperture of 0.5 mm in the newly formed branch of the hydraulic fracture. From Equation DR2-1, this corresponds to a magnitude of –0.64, and thus similar failure characteristics to the real event shown in Figure 3.

Figure 4C shows fluid pressure at an observation point, initially close to the tip of the previous

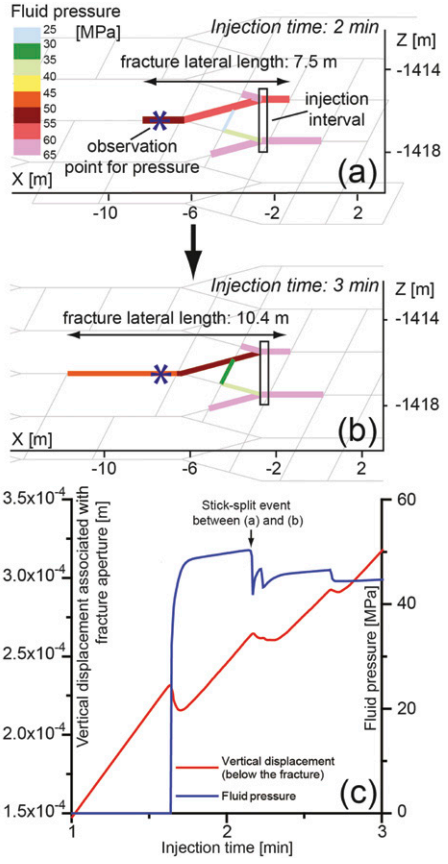

Figure 4. A,B: Two different instants in time illustrating cyclical increase and decrease of fluid pressures at hydraulic fracture tip during fracture propagation. Gray lines are predefined fracture network. Colored lines are fluid pressures. Black box is injection interval within vertical well. C: Temporal variations in fluid pressure (blue line) at observation point (blue star) shown in A and B, and vertical displacement (red line) 9 m below observation point. Fluids reach observation point after 1.6 min. Fluid pressure then builds up until 2.2 min, when failure event shown between A and B occurs. Subsequent cyclic pressure variations indicate episodic fracture growth. Relative variations in vertical displacement capture hydraulic fracture clapping mechanism (opening and closing of walls).

failure event, and the vertical displacement 9 m below this point. The vertical displacement is indicative of the evolution in fracture aperture. Displacement is somewhat damped due to rock elasticity and the distance from the fracture, yet its cyclic variations indicate repeated opening and closing. Likewise, the fluid pressure builds up repetitively until failure, followed by rapid drops due to the newly created fracture volume. Simultaneously, fracture aperture expands during fluid pressure buildup, followed by a subsequent decrease on fracture propagation, revealing the clapping mechanism. For longer injection times, pressure fluctuations at the observation point decrease to a constant level, consistent with the mostly constant fracture propagation pressures seen in many hydraulic fracturing treatments (Zoback, 2007), due to increasing system volume and storativity.

DISCUSSION AND CONCLUSIONS

Geologic, seismic, and numerical observations indicate that stick-split failure is a likely mechanism for anthropogenic fluid-induced failure. Seismic observations also provide direct and indirect measurements of the anticipated fracture lengths and time separations between opening and partial closing at the crack tip. The observations of nearly uniform injection pressures during hydraulic fracturing treatments and continuous growth of the resulting microseismic clouds do not contradict episodic fracture growth, because fracture compliance increases with the cube of its radius (Raaen et al., 2006), suppressing pressure variations measured at the injection point. Moreover, cyclic pressure variations immediately after the formation breakdown pressure are in some cases observed in extended leak-off tests (Raaen et al., 2006), similar to those shown in Figure 4C. Likewise, the growth of the microseismic cloud is measured on time scales of minutes to hours (Shapiro et al., 1997), instead of fractions of seconds, rendering episodic stick-slip growth difficult to resolve using standard methods of analysis.

The maximum size of the microseismic clouds for individual stages of the hydraulic fracturing treatment in central Alberta (Eaton et al., 2014a) is given by $r(t) = 276\ t^{1/2}$, where r is distance from the injection point and t is time (Eaton et al., 2014b). This leads to an upper bound for the tip propagation speeds of 5.6 m/min, 3.3 m/min, and 2.3 m/min at, respectively, 10, 30, and 60 min after the start of each treatment stage. The numerical modeling produces growth rates of 2–5 m/min for the first 10 min of fluid injection, then 0.5–1 m/min between 10 and 30 min of fluid injection, followed by periods of complete growth stagnation. Such propagation velocities more commonly associated with subcritical, continuous fracture growth due to stress corrosion (Anderson and Grew, 1977; Atkinson and Meredith, 1987).

Care should thus be taken not to attribute slow average fracture propagation speeds due to stick-split behavior, where significant time is consumed by halting of the rupture process, to slow, subcritical, continuous fracture growth. In particular the presence of microseismicity in natural rocks, or acoustic emissions in laboratory experiments (P.G. Meredith, 2015, personal commun.), is likely indicative of episodic failure with rupture speeds of individual events on the order of the shear-wave velocity. Indeed, rupture velocities on the order of 10^{-2}–10^{-1} m/s are associated with region III of the subcritical growth process which occurs close to critical stress intensities. This region is thought to represent a combination of mechanical cracking and stress corrosion (Anderson and Grew, 1977).

Stick-split behavior in hydraulic fracturing treatments and stick-slip failure in earthquakes therefore exhibit substantial similarities, in that in both cases the rupture process often temporarily halts (sticks) until sufficient stress has built up to overcome either the tensile rock strength (fracture toughness) by splitting, or the frictional resistance created by asperities and fracture roughness to allow slipping (shearing). Seismic observations thus put a time scale on the stick-split process, e.g., by revealing that the time lag τ between opening and partial closing at the tip is on the order of milliseconds. Given the relatively large time durations spent in the halting stage, it is indeed possible that stress corrosion and subcritical crack growth also occur, even when the stick-split or stick-slip mechanisms are the kinetically most noticeable failure processes.

We anticipate that our findings will lead to enhanced mathematical models describing fluid-induced fracture propagation near the crack tip. Furthermore, our findings may lead to improved insights into (1) natural hydraulic fracturing, in particular on physical and geologic conditions determining episodic, stick-split behavior or continuous joint growth, (2) interaction of a propagating anthropogenic hydraulic fracture with preexisting natural and incipient fractures, which commonly results in very complex fracture zones, and (3) rock-fluid interactions in general.

ACKNOWLEDGMENTS

Van der Baan and Eaton thank the sponsors of the Microseismic Industry Consortium and the Natural Sciences and Engineering Research Council for financial support. Preisig thanks the Swiss National Science Foundation (project no. 146075) for financial support. We thank B. Holdsworth, A. Lacazette, P.G. Meredith, and an anonymous reviewer for their comments and suggestions, in particular on natural hydraulic fracturing (Lacazette), subcritical crack growth in laboratory experiments (Meredith), and effect of fluid compressibility (anonymous reviewer). Rock properties, fracture networks, and stress field data used in Table DR1 are kindly provided by Newcrest, Australia.

REFERENCES CITED

Adachi, J., Siebrits, E., Peirce, A., and Desroches, J., 2007, Computer simulation of hydraulic fractures: International Journal of Rock Mechanics and Mining Sciences Abstract, v. 44, p. 739–757, doi:10.1016/j.ijrmms.2006.11.006.

Aki, K., Fehler, M., and Das, S., 1977, Source mechanism of volcanic tremors: Fluid-driven crack model and their application to the 1963 Kilauea eruption: Journal of Volcanology and Geothermal Research, v. 2, p. 259–287, doi:10.1016/0377-0273(77)90003-8.

Anderson, O.L., and Grew, P.C., 1977, Stress corrosion theory of crack propagation with applications to geophysics: Reviews of Geophysics and Space Physics, v. 15, p. 77–104, doi:10.1029/RG015i001p00077.

Atkinson, B.K., and Meredith, P.G., 1987, The theory of subcritical crack growth with applications to minerals and rocks, *in* Atkinson, B.K., ed., Fracture Mechanics of Rock: London, Academic Press, p. 111–166, doi:10.1016/B978-0-12-066266-1.50009-0.

Bahat, D., and Engelder, T., 1984, Surface morphology and cross-fold joints of the Appalachian Plateau, New York and Pennsylvania: Tectonophysics, v. 104, p. 299–313, doi:10.1016/0040-1951(84)90128-8.

Brace, W.F., and Byerlee, J.D., 1966, Stick-slip as a mechanism for earthquakes: Science, v. 153, p. 990–992, doi:10.1126/science.153.3739.990.

Cipolla, C., Maxwell, S., Mack, M., and Downie, R.A., 2011, Practical guide to interpreting microseismic measurements: Paper SPE 144067, presented at the Society of Petroleum Engineers Americas Unconventional Gas Conference, The Woodlands, Texas, 14–16 June, doi:10.2118/144067-MS.

Cundall, P.A., 1988, Formulation of a three-dimensional distinct element model: Part I. A scheme to detect and represent contacts in a system composed of many polyhedral blocks: International Journal of Rock Mechanics and Mining Sciences & Geomechanics Abstracts, v. 25, p. 107–116, doi:10.1016/0148-9062(88)92293-0.

Davis, G.H., Reynolds, S.J., and Kluth, C.F., 2011, Structural Geology of Rocks and Regions (third edition): Hoboken, New Jersey, John Wiley & Sons, 864 p.

Eaton, D., van der Baan, M., Tary, J.-B., Birkelo, B., Spriggs, N., Cutten, S., and Pike, K., 2013, Broadband microseismic observations from a Montney hydraulic fracture treatment, northeastern B.C., Canada: Canadian Society of Exploration Geophysics Recorder, v. 38, p. 45–53.

Eaton, D., Caffagni, E., Rafiq, A., van der Baan, M., Roche, V., and Matthews, L., 2014a, Passive seismic monitoring and integrated geomechanical analysis of a tight-sand reservoir during hydraulic-fracture treatment, flowback and production: Paper 1929223 presented at Unconventional Resources Technology Conference, Denver, Colorado, 25–27 August, doi:10.15530/urtec-2014-1929223.

Eaton, D., Rafiq, A., Pedersen, P., and van der Baan, M., 2014b, Microseismic expression of natural fracture activation in a tight sand reservoir, *in* Proceedings of the 1st International Conference on Discrete Fracture Network Engineering, 19–22 October, Vancouver, Canada, Paper DFNE 2014–265.

Eaton, D.W., van der Baan, M., Birkelo, B., and Tary, J.-B., 2014c, Scaling relations and spectral characteristics of tensile microseisms: Evidence for opening/closing cracks during hydraulic fracturing: Geophysical Journal International, v. 196, p. 1844–1857, doi:10.1093/gji/ggt498.

Foulger, G.R., and Long, R.E., 1984, Anomalous focal mechanisms: Tensile crack formation on an accreting plate boundary: Nature, v. 310, p. 43–45, doi:10.1038/310043a0.

Lacazette, A., and Engelder, T., 1992, Fluid-driven cyclic propagation of a joint in the Ithaca Siltstone, Appalachian Basin, New York, *in* Evans, B., and Wong, T.-F., eds., Fault Mechanics and Transport Properties of Rocks: A Festschrift in Honor of W.F. Brace: San Diego, California, Academic Press, p. 297–323, doi:10.1016/S0074-6142(08)62827-2.

Preisig, G., Eberhardt, E., Gischig, V., Roche, V., van der Baan, M., Valley, B., Kaiser, P.K., Duff, D., and Lowther, R., 2015, Development of connected rock mass permeability through hydraulic fracture propagation and shearing accompanying fluid injection: Geofluids, v. 15, p. 321–337, doi:10.1111/gfl.12097.

Raaen, A.M., Horsrud, P., Kjørholt, H., and Økland, D., 2006, Improved routine estimation of the minimum horizontal stress component from extended leak-off tests: International Journal of Rock Mechanics and Mining Sciences, v. 43, p. 37–48, doi:10.1016/j.ijrmms.2005.04.005.

Rubin, A.M., 1993, Tensile fracture of rock at high confining pressure: Implications for dike propagation: Journal of Geophysical Research, v. 98, p. 15,919–15,935, doi:10.1029/93JB01391.

Secor, D.T., Jr., 1969, Mechanics of natural extension fracturing at depth in the earth's crust, *in* Baer, A.J., and Norris, D.K., eds., Research in Tectonics: Geological Survey of Canada Paper 68-52, p. 3–48.

Shapiro, S.A., Huenges, E., and Borm, G., 1997, Estimating the crust permeability from fluid-injection-induced seismic emission at the KTB site: Geophysical Journal International, v. 131, p. F15–F18, doi:10.1111/j.1365-246X.1997.tb01215.x.

van der Baan, M., Eaton, D., and Dusseault, M., 2013, Microseismic monitoring developments in hydraulic fracture stimulation, *in* Bunger A.P., McLennan, J., and Jeffrey, R., eds., Effective and Sustainable Hydraulic Fracturing: Rijeka, Croatia, Intech, p. 439–466, doi:10.5772/56444.

Vavryčuk, V., 2011, Tensile earthquakes: Theory, modeling, and inversion: Journal of Geophysical Research, v. 116, B12320, doi:10.1029/2011JB008770.

Walter, W.R., and Brune, J.N., 1993, Spectra of seismic radiation from a tensile crack: Journal of Geophysical Research, v. 98, p. 4449–4459, doi:10.1029/92JB02414.

Zoback, M.D., 2007, Reservoir Geomechanics: Cambridge, UK, Cambridge University Press, 449 p., doi:10.1017/CBO9780511586477.

Manuscript received 23 February 2016
Revised manuscript received 2 May 2016
Manuscript accepted 3 May 2016

Printed in USA